

Characteristics of Significant Wave Components in the Long Time Wave Evolution Process

Shuya Xie^{1,2}, Aifeng Tao^{1,2}, Xue Han³, Xishan Pan³ and Wei Xu^{1,2}

Received: 02 July 2022 / Accepted: 17 October 2022

© Harbin Engineering University and Springer-Verlag GmbH Germany, part of Springer Nature 2023

Abstract

Spectral bandwidth is a relevant parameter of water wave evolution and is commonly used to represent the number of wave components involved in wave–wave interactions. However, whether these two parameters are equivalent is an open question. Following the high-order spectral method and taking the weakly modulated Stokes wave train as the initial condition, the relationship between the spectral bandwidth and the number of wave components is investigated in this work. The results showed that the number of wave components can vary with the same spectral bandwidth and that distinct wave profiles emerge from different numbers of wave components. With a new definition of significant wave components, the characteristics of this parameter in the long-time wave evolution are discussed, along with its relationship with common parameters, including the wave surface maximum and the wave height. The results reveal that the wave surface evolution trend of different numbers of significant wave components (N_s) is the same from a holistic perspective, while the difference between them also exists, mainly in locations where extreme waves occur. Furthermore, there is a negative correlation between r (a/a_0) and wave surface maximum (η_{\max}/a_0) and wave height (H_{\max} and H_s). The evolution trends of the relative errors (RE) of η_{\max}/a_0 , H_{\max} , and H_s of different N_s show the periodic recurrence of modulation and demodulation in the early stage when the Benjamin–Feir instability is dominated. The difference is that in the later stage, the RE of η_{\max}/a_0 and H_{\max} is chaotic and irregular, while those of H_s gradually stabilize near an equilibrium value. Furthermore, we discuss the relationship between the mean relative error (MRE) and r . For η_{\max}/a_0 , MRE and r show a logarithmic relationship, while for H_{\max} and H_s , a quadratic relationship exists between them. Therefore, the choice of N_s is also important for extreme waves and is particularly meaningful for wave generation experiments in the wave flume.

Keywords Spectral bandwidth; Significant wave components; Long-time wave evolution; Wave surface maximum; Maximum wave height

Article Highlights

- The difference between the spectral bandwidth and the number of wave components is investigated, it is of great significance for the study of extreme waves and the wave generation in the wave flume;
- A new parameter “significant wave components (SWC)” is defined;
- Whether different numbers of significant wave components will produce different waves under the same spectral bandwidth are discussed;
- Relationships of significant wave components with several common parameters are discussed.

✉ Aifeng Tao
aftao@hhu.edu.cn

¹ Key Laboratory of the Ministry of Education for Coastal Disaster and Protection, Hohai University, Nanjing 210024, China

² College of Harbour, Coastal and Offshore Engineering, Hohai University, Nanjing 210024, China

³ Tidal Flat Research Center of Jiangsu Province, Nanjing 210036, China

1 Introduction

Spectral bandwidth has an important influence on water wave evolution. Many studies have shown that the occurrence of extreme waves, such as rogue waves, is often accompanied by the phenomenon known as spectral bandwidth enlargement (Dysthe et al. 2003; Tao et al. 2010, 2012, 2021). It means that there are more wave components participating in wave interaction. Therefore, a spectral bandwidth often has the same physical significance as the number of wave components. Such a bandwidth is used by default to represent the number of wave components participating in the action. The larger the bandwidth, the greater the number of component waves. However, whether they are exactly the same constitutes a very interesting research topic. In this paper, we discuss whether

different numbers of wave components will produce different waves under the same spectral bandwidth. Furthermore, we focus on the characteristics of different numbers of wave components in the long-time evolution of wave trains.

Most of the studies on spectral bandwidth and initial wave steepness were conducted via the Benjamin–Feir Index (BFI). Janssen (2003) proposed a combined-parameter BFI to characterize the ratio of wave steepness to spectral bandwidth based on the excitation conditions of modulation instability. He pointed out that when BFI is greater than 1, modulation instability occurs, possibly along with rogue waves. Furthermore, the frequency of such rogue waves will increase with the increase of BFI value. Mori and Janssen (2006) statistically analyzed the occurrence frequency of rogue waves based on this factor, which made the theory further accepted by the public. The quantitative estimation of the evolution characteristics of random wave fields based on BFI is quite common. For example, Onorato et al. (2006) utilized BFI to analyze the relatively wide JONSWAP spectrum. In addition, Onorato et al. (2001) also simulated the evolution of the undirected wave field through the nonlinear Schrödinger equation, proving that modulation instability can significantly change the spectrum and increase the probability of rogue waves. Ma et al. (2012) investigated the effect of dissipation on the evolution of the Benjamin–Feir instability.

Xia et al. (2015) adopted the nonlinear fourth-order Schrödinger equation to simulate the generation of rogue waves characterized by the JONSWAP spectrum. Their results show that BFI is an important parameter that can be used in identifying the existence of instability. Ponce de León and Guedes Soares (2014) studied extreme wave parameters (BFI, kurtosis, and H_{\max}/H_s) of North Atlantic extratropical cyclones and found that under these conditions, BFI and kurtosis increase significantly, mainly in the fourth quadrant. Luxmoore et al. (2019) found that when considering the influence of bound mode, the kurtosis of two-component seas can be well estimated by directional diffusion using the empirical relationship based on BFI. This can then be used to predict the occurrence probability of extreme waves generated by directional propagation under complex sea conditions.

Xiao et al. (2013) studied the generation mechanism and occurrence probability of rogue waves in 3D wave fields based on the high-order spectral method (HOS) and proposed that the modified BFI (MBFI) factor is more advantageous in predicting the occurrence probability of directional seas than BFI. Ruban (2016) proved the fundamental possibility of using a sufficiently small BFI in the linear model to predict in advance the rogue waves of the sea state. Ducroz et al. (2008) studied the formation of extreme waves, especially the effect of nonlinearity (mean steepness or BFI) on these events. Gramstad and Trulsen

(2007) revealed that BFI is a good indicator of an increase in rogue wave activity but only under the condition of long crest length.

Li et al. (2015) studied rogue wave generation in random wave trains. Their results reveal that group height GF_w gradually increases with the development of wave instability. Furthermore, they found no significant relationship between group length GL_w and instability of the wave train and that GL_w mainly depends on the bandwidth of the spectrum. Tang et al. (2020) examined the kurtosis of the linearized free surface as a convenient index for the probability of a rogue wave and proposed that above a certain steepness threshold, the steady-state value of kurtosis mainly depends on spectral bandwidth. Qi (2016) pointed out that in the long-term evolution of the wave train, spectral bandwidth gradually tends to stabilize near an equilibrium value. Doong et al. (2018) proposed a data-driven early warning model based on an artificial neural network to predict the occurrence of coastal rogue waves. They collected seven parameters, namely, significant wave height, peak period, wind speed, wave group coefficient, BFI, kurtosis, and wind direction deviation.

Based on the measured data and the high-order spectral numerical model, Fujimoto et al. (2018) focused on the influence of four-wave resonance on the generation of rogue waves. They speculated that four-wave quasi-resonance and dispersion focusing are the causes of rogue waves, but their relative importance depends on the spectral bandwidth. Meanwhile, Mori (2004) investigated the increase in the occurrence probability of rogue waves due to the fourth-order moment, kurtosis, and change of surface elevation. The results showed that the nonlinear effect on the occurrence probability of rogue waves was actually linear with the kurtosis for a small number of waves. Mori (2003) also focused on the kurtosis of surface elevations due to wave breaking and found that the maximum limit of kurtosis of surface elevations is inhibited by wave breaking. Zheng et al. (2016) adopted the Green–Naghdi models and physical experiments to study the evolution of gravity wave groups with moderate wave steepness. Dong et al. (2019) developed a new nonhydrostatic model to simulate the evolution of unidirectional propagating waves in intermediate and deep waters and further discussed the kinematic characteristics of extreme waves during wave evolution.

Thus far, scholars have conducted in-depth research on the influence of different water wave mechanisms, spectral bandwidth, initial wave steepness, and kurtosis, on rogue waves, among others. However, according to the phenomena we observed, the magnitude of spectral bandwidth is unable to accurately represent the number of significant wave components. In fact, under the condition of the same spectral bandwidth, we found that there are different numbers of significant wave components and wave profiles. Therefore, we investigated the characteristics of significant

wave components and their relationship with several common wave parameters, including wave surface maximum, maximum wave height, and significant wave height.

The remainder of the paper is organized as follows. In Section 2, the description of the long-time evolution model of the weakly modulated Stokes wave train based on the HOS is given, as well as the definitions of the number of significant wave components N_s and the spectral bandwidth B . In Section 3, we discuss and analyze the characteristics of significant wave components (SWC) based on the HOS simulation results, as well as the relationships of these characteristics with wave surface maximum, maximum wave height, and significant wave height. Finally, the conclusions are given in Section 4.

2 Methodology and definitions

2.1 High-order spectral method

The HOS is a phase-resolved numerical model used for simulating water wave evolution. It was developed in 1987 by Dommermuth and Yue (1987) and West et al. (1987). The HOS is a pseudo-spectral and Zakharov-equation-based method that follows the evolution of N wave modes and accounts for their nonlinear interactions up to an arbitrary high order, M . The method obtains exponential convergence with respect to both N and M . Moreover, it combines the advantages of the Fast Fourier Transform algorithm. This method obtains an operation count that is almost linearly proportional to N and M . Due to its high efficiency and accuracy, the HOS is an effective approach for long-time and large-space simulation of nonlinear wave-field evolutions. The details of this method and its valuable applications can be found in many references, such as Wu (2004), Tao (2007), Tao et al. (2012, 2014, 2021), and Xiao et al. (2013).

2.2 Modulated Stokes wave train long time evolution

The initial weakly modulated wave train is constructed by a Stokes carrier wave and imposed sideband according to the most unstable modulation instability condition. For the weakly modulated wave train, the initial conditions we used are as follows:

$$\left. \begin{aligned} \eta(x, 0) &= \eta[\varepsilon_0, k_0] + r_{21}a_0 \cos(k_-x - \theta_-) \\ &\quad + r_{22}a_0 \cos(k_+x - \theta_+) \\ \varphi^s(x, 0) &= -\varphi^s[\varepsilon_0, k_0] + \frac{r_{21}a_0}{\sqrt{k_-}} e^{k_-x} \sin(k_-x - \theta_-) \\ &\quad + \frac{r_{22}a_0}{\sqrt{k_+}} e^{k_+x} \sin(k_+x - \theta_+) \end{aligned} \right\} \quad (1)$$

where $\eta(x, 0)$ and $\varphi^s(x, 0)$ are the free-surface elevation and potential of a right-going Stokes wave of steepness ε_0 and wave number k_0 , respectively. Here $\varepsilon_0 = k_0 a_0$ and a_0 refer to the surface elevation of the carrier wave, while $k_{\pm} = k_0 \pm \Delta k$ and θ_{\pm} are wave numbers and phases of the sideband, respectively. Those parameters are chosen as the most unstable conditions in the initial period. The calculation domain of the whole wave field is 2π , and the wave number k_0 in the calculation domain of 2π is 128. The parameters for HOSM are $M = 7$, $N = 4096$, and $T_0/dt = 64$. Here, dt is the time step for simulation. For the determination of the value of M , please refer to Tao et al. (2021). Similarly, the time length of wave train evolution is $10000T_0$, where T_0 is the period of the carrier wave. The initial wavenumber–amplitude spectrum and corresponding wave surface for $\varepsilon_0 = 0.06$ are shown in Figure 1.

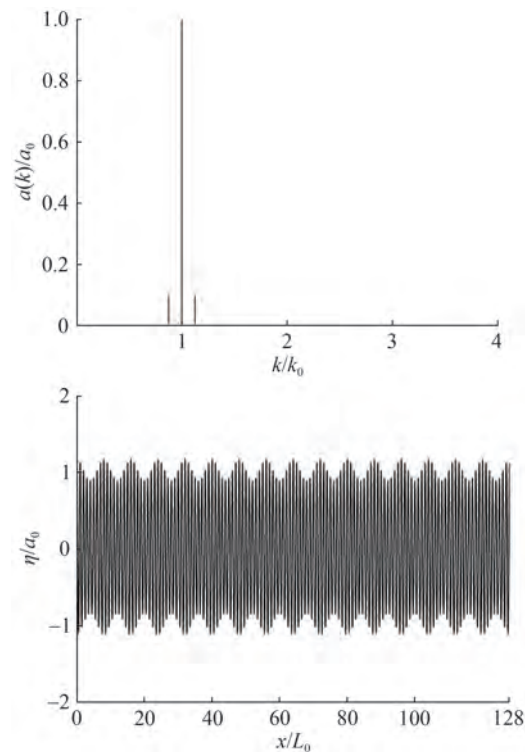


Figure 1 Initial wavenumber–amplitude spectral and wave surface

2.3 Definitions of N_s and B

There is cognition about the number of wave components, but in the numerical model, we have yet to determine the amplitude of the wave that can be used as the wave component involved in wave interaction. This task requires a clear definition. Thus, we propose a new concept: SWC referring to the wave whose amplitude meets a certain requirement, as described below. Meanwhile, the definition of spectral bandwidth B is given below.

2.3.1 Significant wave components

We define N_s as the number of SWC participating in the action. Here, N_s is expressed as:

$$N_s(t) = N_s(t) + 1, \quad \text{if } \frac{a_j(t)}{a_0} \geq r \quad (2)$$

where $a_j(t)$ is the amplitude of the wave component at time t , and a_0 is the amplitude of the carrier wave. In addition, N_s represents the number of SWC participating in the action; that is, a larger N_s means more wave components can take action. The discussions on the value of r will be explained later.

2.3.2 Spectral bandwidth B

In our study, we define spectral bandwidth B as the ratio of the difference between the maximum and minimum wavenumbers in the wavenumber spectrum to the carrier wavenumber. The approach to determining the maximum and minimum wavenumbers is as follows. First, we find wave components whose amplitude to carrier amplitude ratio is greater than the specific value r . Then, to obtain the wave numbers corresponding to these wave components, the maximum and minimum wave numbers are obtained. On the one hand, as the initial condition in our study is discrete spectral rather than continuous random wave spectral, the spectral bandwidth calculation method of random wave spectrum is not applicable. On the other hand, the ratio of the amplitude of the sideband to the amplitude of the carrier is 0.1 in the initial condition; hence, the commonly used definition of the difference between the two wavenumbers corresponding to half of the maximum amplitude is no longer applicable to this. The definition of spectral bandwidth B is shown in Figure 2.

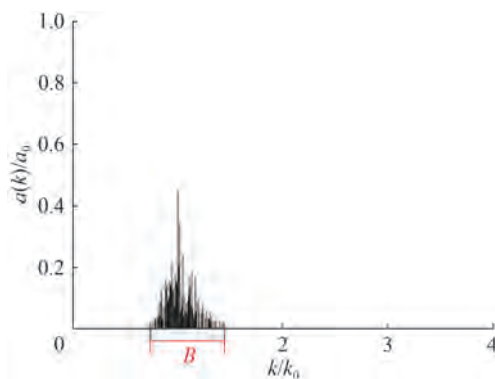


Figure 2 Definition of spectral bandwidth B

We set up ten groups of different values of r ($r = 0.01, 0.02, 0.03, \dots, 0.1$) to explore the characteristics of SWC in the long-time evolution and their relationships with other common parameters.

3 Results and discussions

3.1 Wave profiles with different N_s

Based on the abovementioned initial conditions, there are two different generation mechanisms of rogue waves in the process of the long-term evolution of the Stokes wave train. One is the modulation instability, and another is related to the wave group interaction (Tao et al. 2012). These two mechanisms are illustrated in Figure 3, which shows the evolution of the wave surface maximum for $\varepsilon_0 = 0.06$. Furthermore, the wave surface maximum $\eta_{\max}(t) = \max\{\eta_c(x, t)\}$, which is represented by the dimensionless η_{\max}/a_0 .

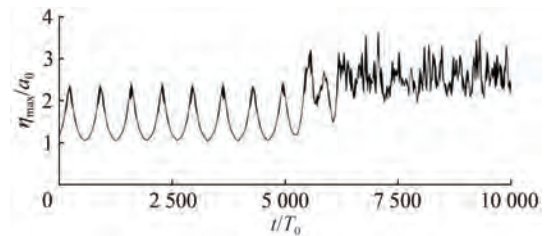


Figure 3 Evolution of wave surface maximum with time

Generally, the spectral bandwidth is used by default to represent the number of wave components participating in the action. The larger the spectral bandwidth, the greater SWC. Figure 4(a) shows the relationship between the number of SWC N_s and spectral bandwidth B in the whole long-time evolution process. However, we find that in the stage of modulation instability, the spectral bandwidth B and the number of SWC N_s are linearly proportional and correspond to each other one by one, as shown in Figure 4(b). At the same time, in Figure 4(c), B and N_s are linearly proportional from $0 < N_s < 10$. In comparison, in the $10 < N_s < 70$ of Figures 4(c) and 4(d), that is, in the stage of transition and wave group interaction, respectively, this phenomenon disappears. There are different numbers of SWC N_s under the condition of the same spectral bandwidth, as shown in Figure 4.

As shown in Figures 5 and 6, on the premise of the same spectral bandwidth, the wave profiles of different N_s are also distinct, regardless of the generation mechanism or evolution stage. Moreover, the larger the N_s , the larger and steeper the wave. In addition, some waves no longer meet the definition of rogue waves after decreasing the number of significant wave components.

3.2 Relationship between N_s and the entire wave surface

The evolution of N_s with time under different r values is presented in Figure 7. As can be seen, the evolution trend

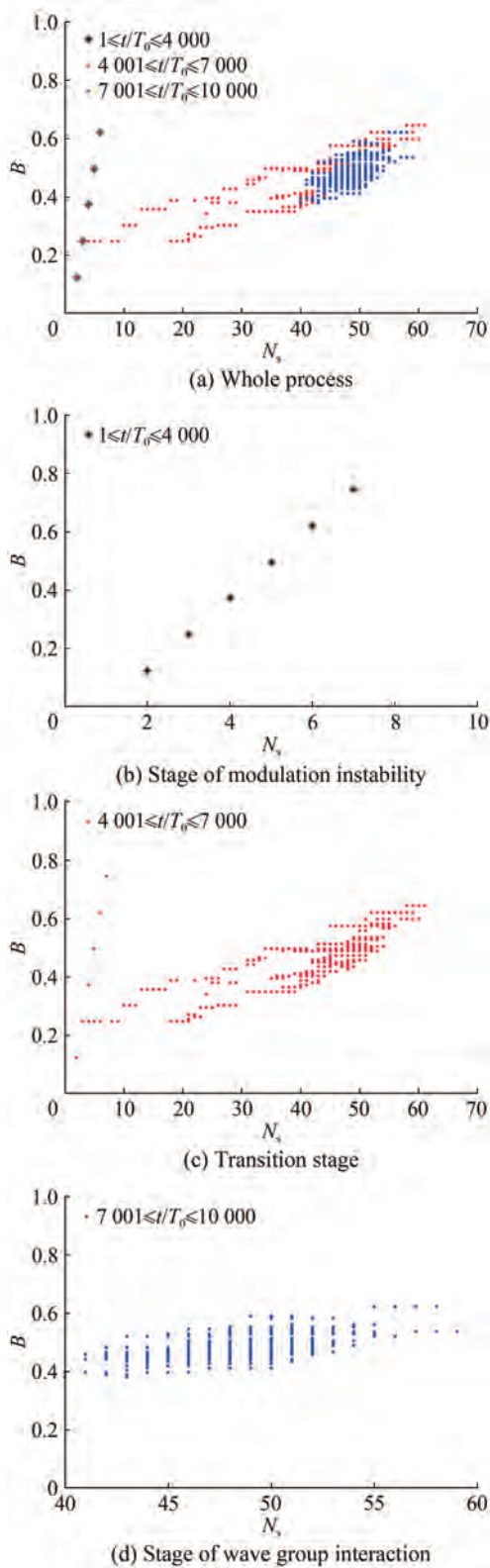


Figure 4 Relationship between N_s and B

of N_s with time is similar to that of the wave surface maximum (Figure 3). Before $t/T_0 \approx O(\varepsilon_0^{-3})$, there is a periodic recurrence similar to the modulation and demodulation

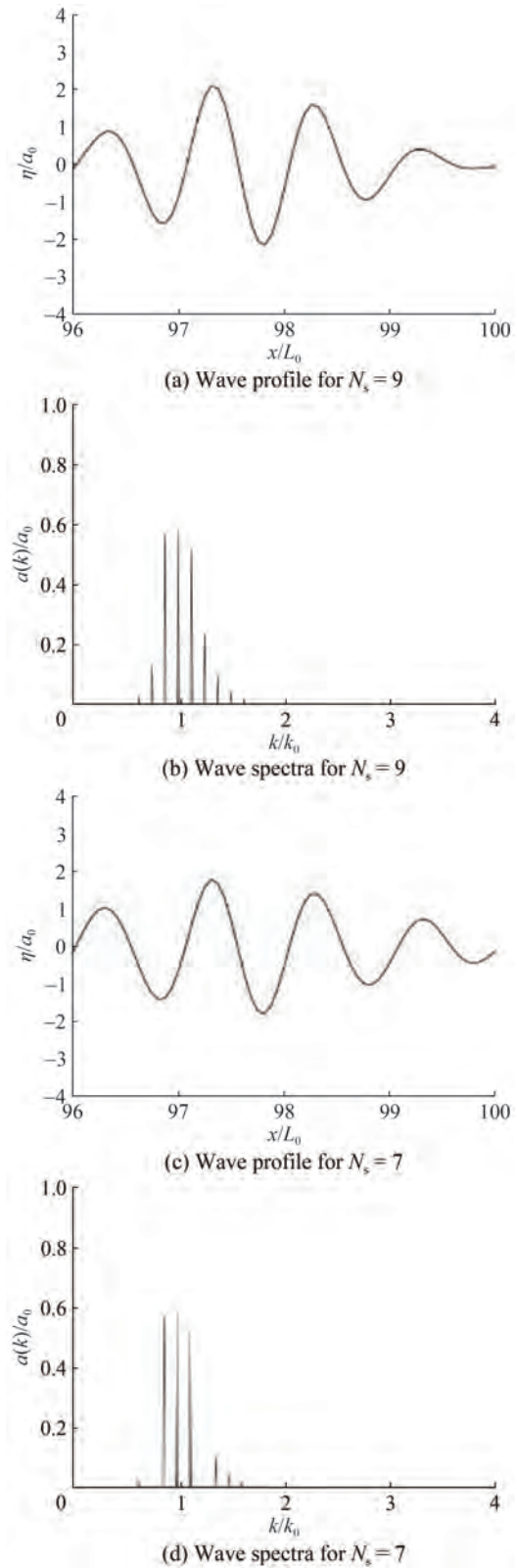


Figure 5 Wave profiles and spectra of different N_s with the same spectral bandwidth at $t/T_0 = 225$

phenomenon. Then, after $t/T_0 \approx O(\varepsilon_0^{-3})$, the periodic recurrence of N_s disappears, after which it enters a chaotic and

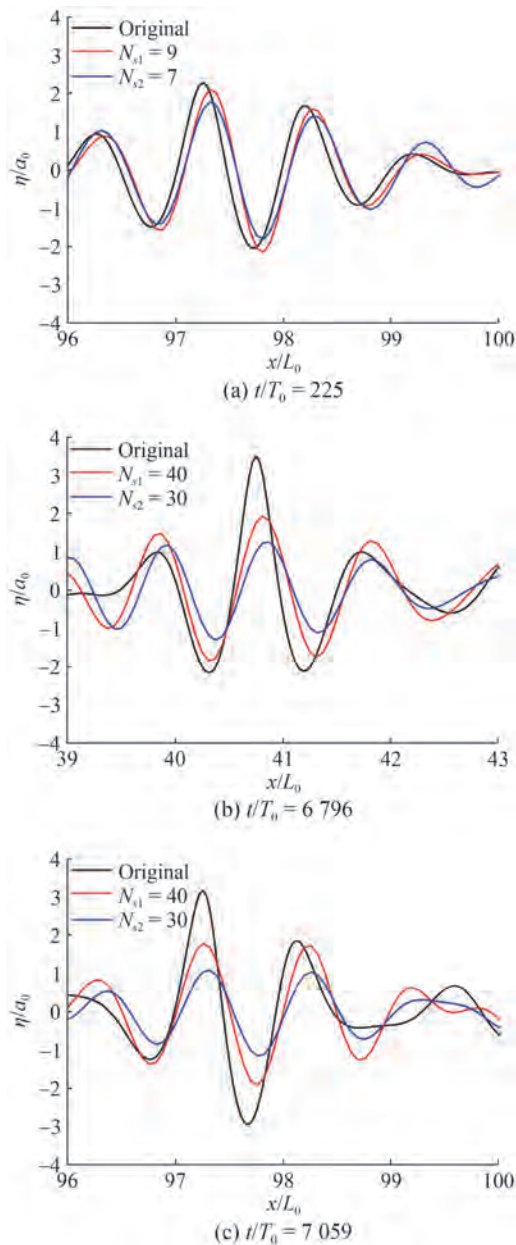


Figure 6 Comparison of wave profiles with different N_s at different times

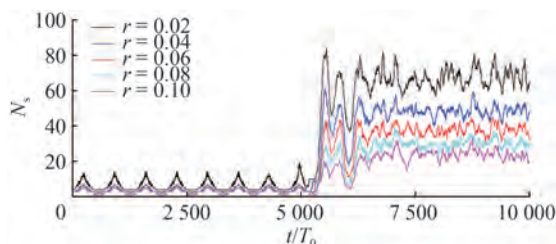


Figure 7 Evolution of N_s with time

irregular state.

To observe the variation of the wave surface more intuitively, we take $r = 0.05$, $t/T_0 = 7.059$ as an example. In

doing so, we can illustrate the comparison between the wave surface generated by the selected SWC and the original wave surface. As shown in Figure 8, the evolution trend of the two wave surfaces is the same. On the whole, the similarity between them is striking, with a correlation coefficient reaching 99.16%. Obviously, the distinct difference between the two wave surfaces is where the rogue wave occurs, and the wave height of the rogue wave decreases significantly.

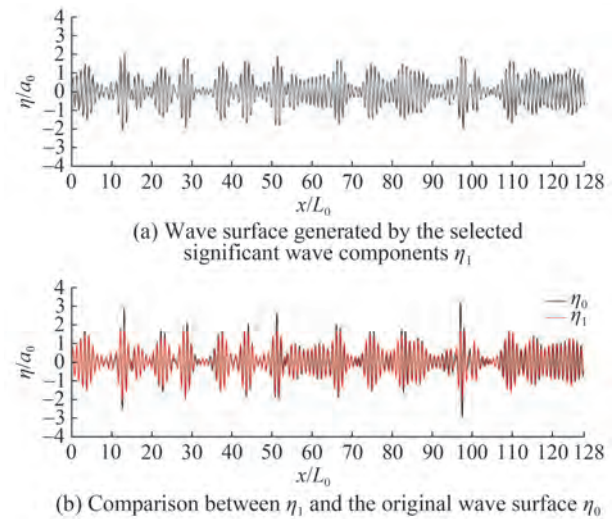


Figure 8 Comparison between the wave surface generated by the selected significant wave components (η_1) and the original wave surface (η_0)

We counted and analyzed the mean relative error (MRE) of the overall wave surface with different r values. The results are shown in Figure 9. As can be seen, the MRE of the overall wave surface is quite small, which means the number of SWC N_s has no significant impact on the evolution of the wave surface from the perspective of the overall wave surface, and can achieve high similarity. Moreover, a quadratic function relation with a correlation coefficient close to 1 is shown in Figure 9 between r and MRE. The fitting formula is shown in Equation (3).

$$\text{MRE} = 364.39r^2 - 2.82r + 0.064 \quad (3)$$

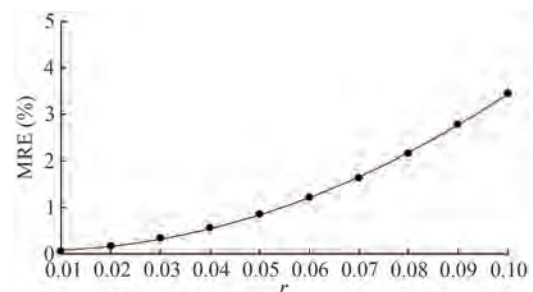


Figure 9 Relationship between r and MRE of the entire wave surface

3.3 Relationship between N_s and the wave surface maximum

The variation of wave surface maximum is very important in the study of rogue waves. Here, we discuss the relationship between N_s and wave surface maximum.

Figure 10 shows the evolution of wave surface maximum with time for different values of r . As can be seen, the evolution trend of wave surface maximum with time is the same under different r values. Before $t/T_0 \approx O(\varepsilon_0^{-3})$, there is a periodic recurrence phenomenon of modulation and demodulation, and after $t/T_0 \approx O(\varepsilon_0^{-3})$, an irregular state emerges. Here, the smaller the value of r , that is, the more SWC, the greater the wave surface maximum.

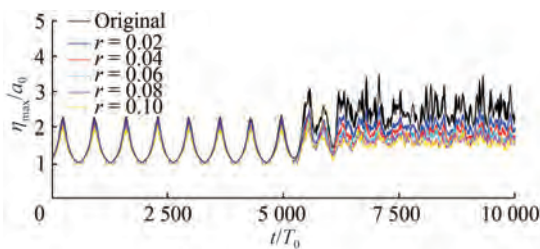


Figure 10 Evolution of wave surface maximum with time for different values of r

As shown in Figure 11, we can obviously see three distinct parts in the correlation between N_s and η_{\max}/a_0 . We speculate that these three parts almost correspond to three different evolution stages: the modulation instability stage, the transition stage, and the wave group interaction stage. Furthermore, there is a positive correlation between η_{\max}/a_0 and N_s , such that the wave surface maximum increases with the increase of N_s .

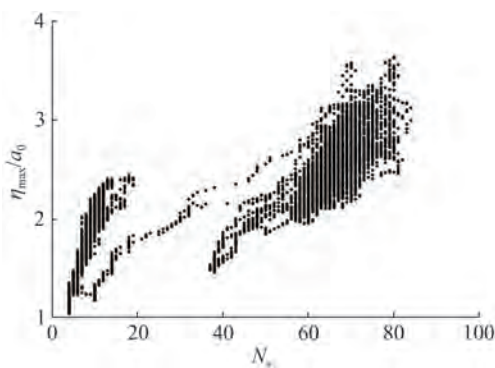


Figure 11 Correlation between N_s and η_{\max}/a_0

Figure 12 shows the evolution of the relative error (RE) of wave surface generated by different N_s with time. As can be seen, the evolution trend of the RE is consistent with that of the wave surface maximum. Before $t/T_0 \approx O(\varepsilon_0^{-3})$, the values of RE are small and are much less than

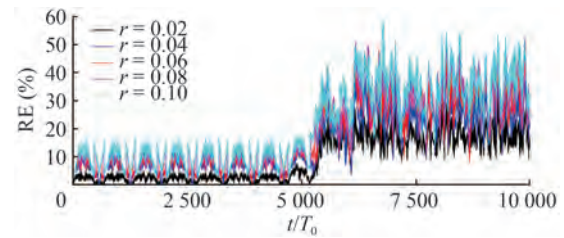


Figure 12 Evolution of the relative error (RE) of wave surface maximum for different r

20%. As the evolution reaches the late stage, the value of RE increases significantly, along with the range. Meanwhile, compared with the whole wave surface, the RE of the wave surface maximum increases obviously. Moreover, there is a positive correlation between RE and r .

Furthermore, the relationship between r and the MRE of the wave surface maximum is obtained, as shown in Figure 13. The results show a logarithmic relationship between the r and the MRE of the wave surface maximum. The correlation coefficient is above 0.99, and the fitting formula is shown in Equation (4):

$$\text{MRE} = 6.73 \ln(r) + 36.22 \quad (4)$$

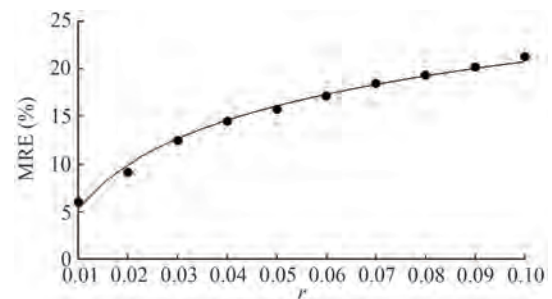


Figure 13 Relationship between r and MRE of wave surface maximum

The number of SWC N_s has an important influence on the magnitude of the wave surface maximum. We can choose the appropriate value of r according to different accuracy requirements. Thus, if we need to control the RE within 10%, the value of r should not be greater than 0.02.

3.4 Relationship between N_s and wave height

Wave height is the most basic characteristic of waves. To further investigate the characteristics of SWC, we conduct further analysis based on the maximum wave height H_{\max} and the significant wave height H_s .

3.4.1 Maximum wave height H_{\max}

As shown in Figure 14, the evolution characteristics of the maximum wave height H_{\max} with time are consistent with that of the wave surface maximum. In the early stage, it is the periodic recurrence of modulation and demodulation,

while in the later stage, it enters an irregular state. Furthermore, the results indicate that a negative correlation exists between H_{\max} and r .

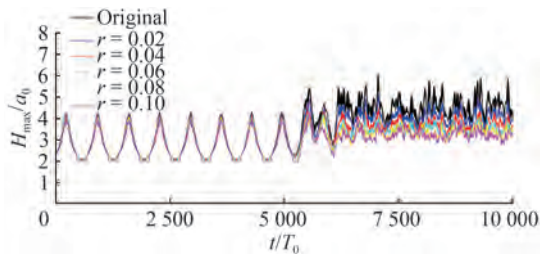


Figure 14 Evolution of H_{\max} with time for different values of r

The evolution of the RE of H_{\max} generated by different N_s with time in Figure 15 is given. Its evolution trend is the same as that of the RE of the wave surface maximum. Similarly, we discuss the relationship between r and MRE, and a quadratic function relation with a correlation coefficient above 0.99 exists between them, as shown in Figure 16. The fitting formula is shown in Equation (5):

$$\text{MRE} = -857.2r^2 + 234.47r + 0.73 \quad (5)$$

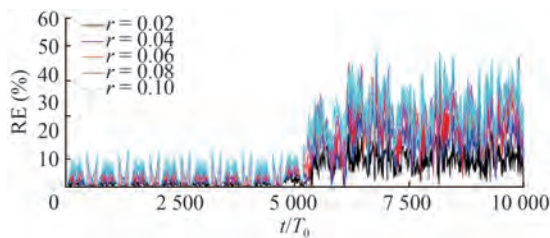


Figure 15 Evolution of the RE of H_{\max} for different values of r

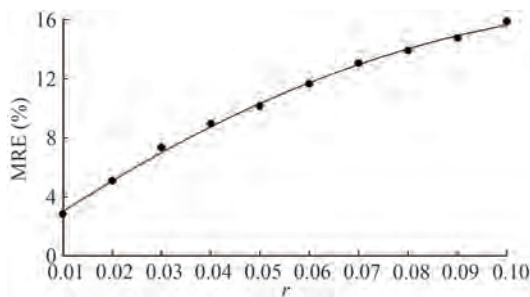


Figure 16 Relationship between r and MRE of H_{\max}

After the above analysis of the relationship between N_s and H_{\max} , we come up with preliminary judgment and valuable suggestions for the determination of r . For H_{\max} , if the RE is kept within 10%, the value of r should be less than 0.04.

3.4.2 Significant wave height H_s

Generally, a wave with more than twice the significant wave height H_s is defined as a rogue wave, so the significant wave height is of great significance in the identification

of rogue waves. The evolution of H_s with time for different r is presented in Figure 17. Compared with the evolution of η_{\max}/a_0 and H_s , in the stage dominated by modulation instability, the variation of H_s with time presents the phenomena of periodic modulation and demodulation recurrence. The difference is that in the stage of wave group interaction, H_s gradually tends to be stable near a certain value and does not enter an irregular state like η_{\max}/a_0 and H_{\max} .

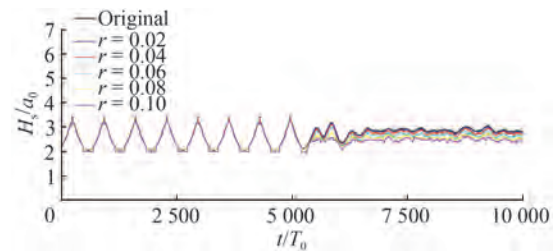


Figure 17 Evolution of H_s with time for different r

The evolution of the RE of H_s generated by different N_s with time is given in Figure 18. It is found that when $r < 0.04$, RE does not vary significantly with time, and its entirety is in a fluctuating equilibrium state with several large values. When $r > 0.04$, there is a trend similar to the variation of the RE of η_{\max}/a_0 and H_{\max} with time. In the early stage, the reoccurrence of modulation and demodulation is observed, while in the later stage, an irregular state emerges. However, in the stage before $t/T_0 \approx O(\varepsilon_0^{-3})$, the MRE is slightly greater than that of the wave surface maximum and the maximum wave height at this stage. Similarly, a quadratic function relation with a correlation coefficient above 0.99 is observed between r and MRE, as shown in Figure 19. The fitting formula is shown in Equation (6):

$$\text{MRE} = 507.95r^2 + 27.37r - 0.0018 \quad (6)$$

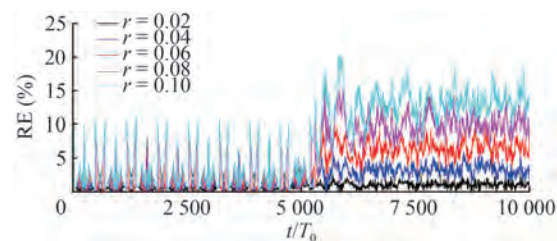


Figure 18 Evolution of the RE of H_s for different values of r

Based on the analysis, we find that the RE of H_s is smaller than that of H_{\max} , in which the value of r has no significant impact on H_s of the wave train. Therefore, the determination of the value of r must be combined with the value of r under the conditions of the wave surface maximum and the maximum wave height.

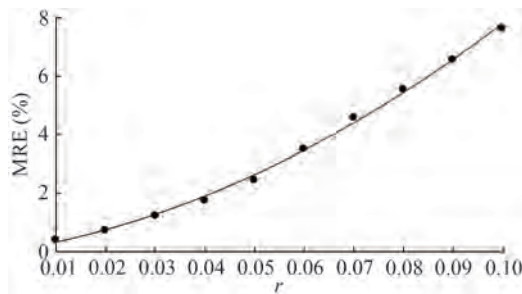


Figure 19 Relationship between r and MRE of H_s

4 Conclusions

Based on the HOS, the characteristics of SWC in the long-time evolution process and their relationships with several common parameters are discussed and analyzed using the weakly modulated Stokes wave train as the initial condition. Several conclusions are obtained as follows.

1) The wave profiles are distinct under the condition of the same spectral bandwidth. Thus, it may not be sufficient to express the number of wave components involved in the action only by using spectral bandwidth. The wave surface evolution trends of different N_s are all the same from a holistic perspective. While differences among them also exist, they only do so in places where extreme waves occur. In other words, the choice of N_s is also important for extreme waves and is particularly meaningful for the wave generation experiments in the wave flume.

2) A negative correlation exists between r and the wave surface maximum η_{\max}/a_0 . The evolution trend of the RE of the wave surface maximum with time is consistent with that of the wave surface maximum. In the early stage, there is a periodic recurrence phenomenon similar to modulation and demodulation, and in the later stage, it enters an irregular state. Moreover, there is a logarithmic relationship between MRE and r . Thus, if the RE of the wave surface maximum is to be kept within 10%, then the value of r should not be greater than 0.02.

3) The evolution trend of H_{\max} with time is the same as η_{\max}/a_0 . Similar to the η_{\max}/a_0 , the evolution trend of the RE of H_{\max} with time is consistent with that of η_{\max}/a_0 . Furthermore, a quadratic relationship exists between MRE and r . Thus, if the RE of H_{\max} is not more than 10%, then the value of r should be less than 0.04.

4) The variation of H_s with time presents periodic modulation and demodulation recurrence phenomenon at the early stage, while it gradually tends to be stable near a certain value in the later stage. The evolution trend of the RE of H_s with time is consistent with that of H_{\max} . Furthermore, a quadratic relationship exists between MRE and r . Finally, for H_s , the determination of r needs to be combined with the value of r of η_{\max}/a_0 and H_{\max} .

Funding Supported by the National Key Research and Development

Program of China (Grant No. 2022YFE0104500), the National Natural Science Foundation of China (Grant No. 52271271), and the Major Science and Technology Project of the Ministry of Water Resources of the People's Republic of China (Grant No. SKS-2022025).

References

- Dommermuth DG, Yue DKP (1987) A high-order spectral method for the study of nonlinear gravity waves. *Journal of Fluid Mechanics* 184: 267-288. DOI: 10.1017/s002211208700288x
- Dong G, Fu R, Ma Y, Fang K (2019) Simulation of unidirectional propagating wave trains in deep water using a fully non-hydrostatic model. *Ocean Engineering* 180: 254-266. DOI: 10.1016/j.oceaneng.2019.03.037
- Doong DJ, Peng JP, Chen YC (2018) Development of a warning model for coastal freak wave occurrences using an artificial neural network. *Ocean Engineering* 169: 270-280. DOI: 10.1016/j.oceaneng.2018.09.029
- Ducrozet G, Bonnefoy F, Ferrant F (2008) Analysis of freak wave formation with large scale fully nonlinear high order spectral simulations. 2008 International Offshore and Polar Engineering Conference, Vancouver, 47-54
- Dysthe KB, Trulsen K, Krogstad HE, Socquet-Juglard H (2003) Evolution of a narrow-band spectrum of random surface gravity waves. *Journal of Fluid Mechanics* 478: 1-10. DOI: 10.1017/s0022112002002616
- Fujimoto W, Waseda T, Webb A (2018) Impact of the four-wave quasi-resonance on freak wave shapes in the ocean. *Ocean Dynamics* 69(1): 101-121. DOI: 10.1007/s10236-018-1234-9
- Gramstad O, Trulsen K (2007) Influence of crest and group length on the occurrence of freak waves. *Journal of Fluid Mechanics* 582: 463-472. DOI: 10.1017/s0022112007006507
- Janssen PAEM (2003) Nonlinear four-wave interactions and freak waves. *Journal of Physical Oceanography* 33(4): 863-884. DOI: 10.1175/1520-0485(2003)33<863:Nfiafw>2.0.Co;2
- Li J, Yang J, Liu S, Ji X (2015) Wave groupiness analysis of the process of 2D freak wave generation in random wave trains. *Ocean Engineering* 104: 480-488. DOI: 10.1016/j.oceaneng.2015.05.034
- Luxmoore JF, Ilic S, Mori N (2019) On kurtosis and extreme waves in crossing directional seas: a laboratory experiment. *Journal of Fluid Mechanics* 876: 792-817. DOI: 10.1017/jfm.2019.575
- Ma Y, Dong G, Perlin M, Ma X, Wang G (2012) Experimental investigation on the evolution of the modulation instability with dissipation. *Journal of Fluid Mechanics* 711: 101-121. DOI: 10.1017/jfm.2012.372
- Mori N (2003) Effects of wave breaking on wave statistics for deep-water random wave train. *Ocean Engineering* 30(2): 205-220. DOI: 10.1016/S0029-8018(02)00017-3
- Mori N (2004) Occurrence probability of a freak wave in a nonlinear wave field. *Ocean Engineering* 31(2): 165-175. DOI: 10.1016/s0029-8018(03)00119-7
- Mori N, Janssen PAEM (2006) On kurtosis and occurrence probability of freak waves. *Journal of Physical Oceanography* 36(7): 1471-1483. DOI: 10.1175/Jpo2922.1
- Onorato M, Osborne AR, Serio M, Bertone S (2001) Freak waves in random oceanic sea states. *Physical Review Letters* 86(25): 5831-5834. DOI: 10.1103/PhysRevLett.86.5831
- Onorato M, Osborne AR, Serio M, Cavaleri L, Brandini C, Stansberg

- C (2006) Extreme waves, modulational instability and second order theory: wave flume experiments on irregular waves. *European Journal of Mechanics-B/Fluids* 25(5): 586-601. DOI: 10.1016/j.euromechflu.2006.01.002
- Ponce de León S, Guedes Soares C (2014) Extreme wave parameters under North Atlantic extratropical cyclones. *Ocean Modelling* 81: 78-88. DOI: 10.1016/j.ocemod.2014.07.005
- Qi K (2016) Long-term evolution of modulated Stokes wave trains and its associated freak wave characteristics. Master thesis, Hohai University, Nanjing, 46-56. (in Chinese)
- Ruban VP (2016) Predictability of the appearance of anomalous waves at sufficiently small Benjamin-Feir indices. *JETP Letters* 103(9): 568-572. DOI: 10.1134/S0021364016090083
- Tang T, Xu W, Barratt D, Bingham HB, Li Y, Taylor PH, Van Den Bremer TS, Adcock TAA (2020) Spatial evolution of the kurtosis of steep unidirectional random waves. *Journal of Fluid Mechanics* 908: A-3. DOI: 10.1017/jfm.2020.841
- Tao A (2007) Nonlinear wave trains evolution and Freak wave generation mechanisms in deep water. PhD thesis, Hohai University, Nanjing, 22-35. (in Chinese)
- Tao A, Qi K, Zheng J, Peng J, Wu Y (2014) The occurrence probabilities of rogue waves in different nonlinear stages. 34th International Conference on Coastal Engineering 2014, Seoul, 1(34): 35. DOI: 10.9753/icce.v34.waves.35
- Tao A, Xie S, Wu D, Fan J, Yang Y (2021) The effects on water particle velocity of wave peaks induced by nonlinearity under different time scales. *Journal of Marine Science and Engineering* 9: 748. DOI: 10.3390/jmse9070748
- Tao A, Yan Y, Zheng J, Zhang W (2010) Characteristics of Stokes wave train long time evolution. Chinese-German Joint Symposium on Hydraulic and Ocean Engineering, Tianjin, 284-287.
- Tao A, Zheng J, Chen B, Li H, Peng J (2012) Properties of freak waves induced by two kinds of nonlinear mechanisms. 33rd International Conference on Coastal Engineering 2012, Santander, Spain
- West BJ, Brueckner KA, Janda RS, Milder DM, Milton RL (1987) A new numerical method for surface hydrodynamics. *Journal of Geophysical Research* 92(C11): 11803-11824. DOI: 10.1029/JC092iC11p11803
- Wu G (2004) Direct simulation and deterministic prediction of large scale nonlinear ocean wave field. PhD Thesis, Massachusetts Institute of Technology, Cambridge, USA
- Xia W, Ma Y, Dong G (2015) Numerical simulation of freak waves in random sea state. *Procedia Engineering* 116: 366-372. DOI: 10.1016/j.proeng.2015.08.300
- Xiao W, Liu Y, Wu G, Yue DKP (2013) Rogue wave occurrence and dynamics by direct simulations of nonlinear wave-field evolution. *Journal of Fluid Mechanics* 720: 357-392. DOI: 10.1017/jfm.2013.37
- Zheng K, Zhao B, Duan W, Ertekin R, Chen X (2016) Simulation of evolution of gravity wave groups with moderate steepness. *Ocean Modelling* 98: 1-11. DOI: 10.1016/j.ocemod.2015.12.003